



Full length article

Assessing food–energy–water resources management strategies at city scale: An agent-based modeling approach for Cape Town, South Africa



Ke Jack Ding^{a,c,*}, Jonathan M. Gilligan^{b,c}, Y.C. Ethan Yang^d, Piotr Wolski^e, George M. Hornberger^{a,b,c}

^a Civil and Environmental Engineering, Vanderbilt University, USA

^b Earth and Environmental Sciences, Vanderbilt University, USA

^c Vanderbilt Institute for Energy and Environment, Vanderbilt University, USA

^d Civil and Environmental Engineering, Lehigh University, USA

^e Climate System Analysis Group, University of Cape Town, South Africa

ARTICLE INFO

Keywords:

Food–energy–water Nexus

Demand-side management

Drought mitigation

Cape Town, South Africa

Agent-based model

Coupled human–natural system model

ABSTRACT

The impact of human activities and climate change occurs across a range of spatial and temporal scales, and the city or regional scale is critical for managing food–energy–water (FEW) resources. We develop a coupled human–natural system model for Cape Town, South Africa, which consists of an agent-based model and a regional hydrologic model, to study the FEW nexus connecting the agricultural, urban, and hydroelectric generation sectors. We use the model to compare three policies—a simple adaptive approach, adaptation with free water to indigent households, and water supply augmentation—and assess their ability to provide reliable FEW services to the different stakeholders under four different climate scenarios, representing moderate to severe amounts of warming. Our results indicate that Cape Town is likely to face increasing water stress as temperatures rise, and that adaptation strategies could effectively mitigate the effects of water limitations and avoid severe failures in providing FEW services across sectors. One way to manage demand for FEW services is by adjusting water price tariffs, but high prices create inequality in access to water for households with different incomes. Our analysis suggests that the water supply system in Cape Town may already be at, if not over, its sustainable capacity within the FEW nexus. Our model serves as a test-bed for assessing policies to manage stresses on water resources for the benefit of stakeholders across FEW sectors. This model can be adapted to cities and regions around the globe.

1. Introduction

Approximately 70% of the world's population is expected to live in an urban setting by 2050 (United Nations, 2018). Delivering adequate food, energy, and water (FEW) services will become increasingly challenging as urban populations keep rising (Zhang et al., 2019). Ensuring meeting the ever-increasing demand of FEW resources for the future is among the top priorities for societies around the globe; careful planning of the utilization of resources is required. Climate change makes such planning even harder because it affects both the availability and the variability of the global and local FEW resources. Climate change also drives the transformation of societies, as they adapt to emerging and future changes and to attempt to mitigate climate change by reducing greenhouse gas emissions to mitigate climate change itself. A sustainable future with sufficient FEW resources needs to take both societal

activities and climate change into consideration.

The FEW nexus can be assessed at various scales, which address different research interests. Previous policy-oriented research on the FEW nexus has mainly focused on factors that influence the dynamics of the nexus (i.e., processes, interrelationships, and outcomes) at larger scales ranging from global and continental levels to the national level. For example, previous research has utilized regression techniques to link FEW resources and services to specific factors such as greenhouse gases and agricultural sustainability in sub-Saharan Africa (SSA) (Ozturk, 2017; Zaman et al., 2017). Ding et al., (2019) used a FEW Resources-Services-Health framework to explore the internal and external factors that influence the interrelationships of resources-to-services and services-to-health of the FEW nexus, in which they found that governance and socio-economic factors, rather than the lack of resources, most significantly influence the FEW services and

* Corresponding author at: Civil and Environmental engineering, Vanderbilt University, Nashville, Tennessee, USA.

E-mail address: ke.ding@vanderbilt.edu (K.J. Ding).

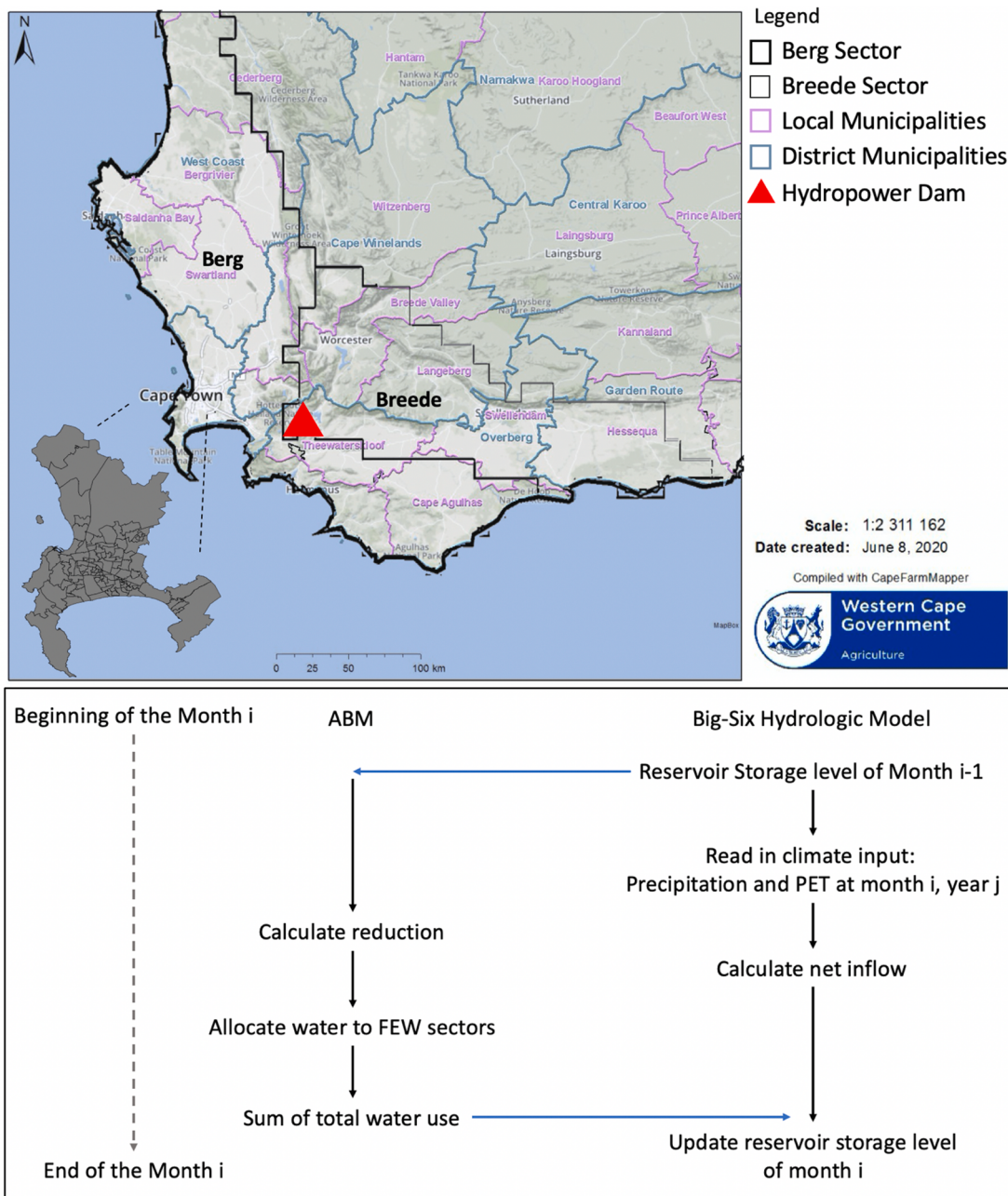


Fig. 1. FEW stakeholders and the coupling mechanism of the human-natural system model. Upper part highlights multiple stakeholders of Food–energy–water sectors in Cape Town regions. Berg and Breede river catchments are the two sectors of the “Big Six” reservoirs system. Wine regions included in this study are Breede Valley, Cape Town, Drakenstein, Langeberg, Stellenbosch, Swartland, and Witzenberg. The vineyard irrigation of the seven wine regions represents the food sector. Cape Town has 116 wards as seen in the grey map at the lower left corner. For the urban water sector, we represent the urban water users in 94 representative wards. The Steenbras upper hydropower dam (red triangle) represents the energy sector in Cape Town. Lower part of the figure illustrates the coupling mechanism of the agent-based model and the Big-Six hydrologic model. The information exchanged between two models are highlighted by the blue arrows.

health in SSA. [Susnik \(2018\)](#) demonstrated the connection between GDP and each of the FEW sectors using global data collected at the national level.

Research on FEW issues at the national scale has identified important relationships, but much of the decision-making apparatus related to allocation and distribution of resources occurs at smaller spatial scales. For example, cities are central to the operation of FEW services as they are where the services are primarily produced, provided, and consumed ([Lant et al., 2019](#)). Therefore, it is important to study and address the challenges of FEW activities, or providing FEW services, at the city level.

For instance, studies have used urban metabolism and life cycle analyses to quantify the fluxes of energy, water, and nutrients to further assess the costs and benefits of specific infrastructural and technological policy implementations ([Heard et al., 2017](#); [Villaruel Walker et al., 2014](#)). Such approaches could be particularly successful in urban areas where data is abundant, but the data constraint limits the applicability to the study regions ([Heard et al., 2017](#); [Villaruel Walker et al., 2014](#)).

In urban systems that suffer from resource deficiency, we argue that more versatile and adaptive methods that could assess policies to optimize the utility of limited FEW resources are needed. Additionally, each

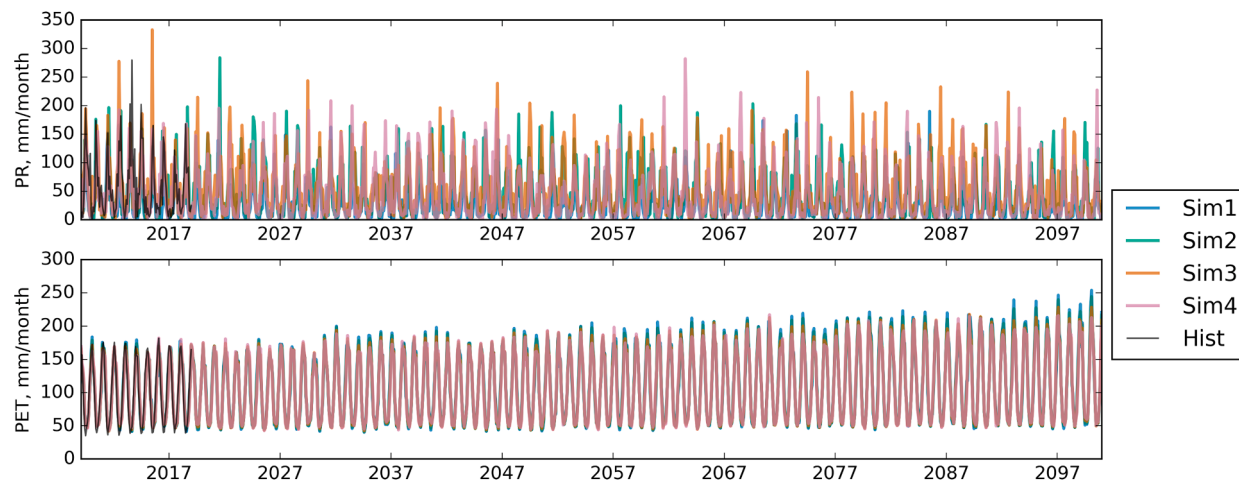


Fig. 2. average precipitation (PR) and calibrated potential evapotranspiration (PET) of different climate scenarios from 2009 to 2100. Sim 1, 2, 3, and 4 correspond to the four climate scenarios realized by climate models M1-4, respectively. Hist represent the values from observation or calculated using observations from 2009 to 2018.

urban area may need responses to FEW stress that are tailored to their own unique conditions and constraints such as local politics, legal and regulatory codes, availability of natural resources, economic conditions, and so forth. For example, more affluent and energy-rich regions can trade a large amount of energy for desalinated water, as seen in Singapore and Dubai (DEWA, 2018; PUB, 2020). Cities draw upon food, energy, and water resources from much larger regions than just the metropolitan area, so urban-rural and urban-urban interconnections both within and across regions must be considered. Watersheds extend far beyond urban boundaries, and at larger scales inter-basin transfer projects can divert water from water-abundant regions to more arid regions, as seen in the United States and China (Shumilova et al., 2018). To ensure sustainable and sufficient supply of FEW resources under future climate uncertainties and with growing population and demand, we need new methods to systematically assess the FEW system outcomes and to evaluate tradeoffs and benefits of different management policies.

FEW nexus models build at such mesoscale has demonstrated their ability to simulate and assessing sector interactions, system outcomes, resources accounting and management, and future climate conditions. More specifically, agent-based modeling (ABM) that includes resource accounting has emerged as a promising method for simulating the performance of urban or regional FEW systems under the influence of both human and natural aspects of the systems while taking heterogeneities among different sectors and stakeholders into account in decision-making (Ding et al., 2019; Hyun et al., 2019; Kanta & Zechman, 2014; Wang et al., 2021; Yang et al., 2018). Cities usually get their water, energy, and food supplies from outside of their political boundaries. Understanding this system thus requires us to couple a model of the urban system to a regional scale model. Recent work using down-scaled regional climate models to project future climate at the local and regional level has enabled higher-resolution studies of the local effects of climate change (Naik & Abiodun, 2019). In this study, we introduce a novel coupled model consisting of an ABM simulating water policy and demand, coupled to a hydrological model for the Cape Town region and apply this to studying challenges to the sustainability of regional FEW resources under different policy scenarios and under future regional climate conditions drawn from multiple downscaled global climate model projections.

We chose Cape Town and Western Cape Province in South Africa as the locale for this model because it represents a complex FEW system

comprising more than 3.8 million people, economically important vineyards, and hydropower installations that supply peak demand to the power grid (Fig. 1), and it faces serious FEW insecurity challenges. Motivated by the recent “Day-Zero” drought crisis (Visser, 2018), our previous study considered a simple ABM with lumped geographical and agent representation and demonstrated that a simple adaptation policy, as oppose to “business as usual”, could significantly improve the services and avoid FEW system failures (Ding et al., 2019). In this study, we expand our analysis of Cape Town to a coupled human-natural system model by coupling our ABM with a regional hydrologic model to examine the water usage across multiple FEW sectors—urban freshwater, vineyards irrigation, and hydropower generation (Fig. 1)—each of which has different impacts on management decisions. We disaggregate the urban sector into water users across the residential regions (the regions where water usage data is collected at) and regroup and represent them in 94 wards (smallest level of administrative divisions in South Africa where census data is reported at) with varying economic conditions and other institutional water users, including government, business, and industry. We take advantage of the agent-based structure of the model to represent the urban sector as a heterogeneous collection of 94 agents, each representing a different ward and characterized by that ward’s water demand and median socio-economic status. Since 94 agents reacts differently to a price tariff based on their initial water demand and their income status, we can use our ABM model to assess the overall performance of the FEW system through their indirect interactions via withdrawals from the common-pool resources. We use this coupled human-natural system model to study how climate change may affect Cape Town’s water supply and the water consumption of urban dwellers, vineyard farming, and the power generation of a hydropower dam out to 2100 under different climate scenarios from moderate to severe. We also use the analysis to test how different policies can affect the city’s ability as a whole to provide sufficient FEW resources and ensure steady water supply for other sectors, and to explore any side effects of those policies such as affordability of water to municipal users across the economic spectrum. Here we focus on the water supply system in Cape Town, nonetheless, the FEW nexus was assessed through the withdrawal of water from the common poll by stakeholders in the food, energy, and water sectors. Our study focuses in particular on the role of reservoirs in storing and supplying water during drought periods. We address the following three hypotheses, each of which we investigate

Table 1
details of the four climate model ensemble members.

Model No.	GCM/RCM	Period of global warming levels			
		1.5°C	2°C	2.5°C	3°C
M1	CanESM2/RCA4	1999-2028	2012-2041	2024-2053	2034-2063
M2	EC-EARTH-1/RCA4	2003-2032	2021-2050	2035-2064	2046-2075
M3	CNRM-CM5/RCA4	2015-2044	2029-2058	2041-2070	2052-2081
M4	GFDL-ESM2M/RCA4	2020-2049	2037-2066	2052-2081	2066-2095

with a different resource planning and management policy under four different climate scenarios.

Hypothesis 1. a simple climate adaptation policy can provide enough water for the operation of the hydropower dam and reasonable prices for the urban dwellers (urban water sector) and the vineyard farmers (agricultural sector) in the Cape Town region, but that this will produce large economic disparities in access to water for drinking and basic hygiene.

Policy 1- simple adaptive approach: proactively raises water tariffs to reduce water demand when the monthly reservoir storage falls below a threshold

Hypothesis 2. providing a basic quantity of water without charge to indigent households can alleviate economic disparities in access to the necessary levels of water for hygiene and drinking while maintaining adequate reservoir storage for reliable hydropower generation.

Policy 2 follows Policy 1 except that indigent households are not charged for the first 6kL per month of consumption.

Hypothesis 3. A water augmentation policy proposed by the Cape Town government can outperform the previous policies at meeting the needs of all sectors—the urban water sector, the agricultural sector, and the energy sector—under expected economic and population growth.

Policy 3- Supplement demand-management by expanding the water supply, including groundwater extraction, wastewater reuse, and desalination.

2. Materials and methods

In this study, we developed a coupled model of the natural and human aspects of the FEW system as a testbed for comparing different management policies in the city of Cape Town. The coupled model consists of two parts: an agent-based model of water demand and management, which we adapted and refined from our previous paper (Ding et al., 2019), and a local hydrologic model of the “Big Six” reservoir system (Climate System Analysis Group, 2019) used by local authority. We used historical climate data to calibrate the model (Fig. 2). To simulate future climates, we selected simulated climate data from four downscaled global climate models under Representative Concentration Pathway (RCP) 8.5 (Naik & Abiodun, 2019). We recognize that RCP 8.5 is an extreme emissions scenario that represents a very unlikely, perhaps even implausible, climate future under anticipated technological, social, economic, and policy scenarios; however, this was the only emissions trajectory for which downscaled model output was available (Hausfather & Peters, 2020; Ritchie & Dowlatabadi, 2017). Rather than following the climate model results as an expected trajectory over the next 80 years, we followed the approach of Naik and Abiodun (2019) and extracted 30-year periods with different mean temperature change relative to estimated preindustrial conditions: 1.5°C (least severe), 2.0°C, 2.5°C, and 3.0°C (most severe). This approach is justified because

both transient and long-term climate change depend far more on cumulative greenhouse gas emissions than on the exact trajectory of emissions over time (Allen et al., 2009; Goodwin et al., 2015). This approach enables us to compare the results of different model realizations of four scenarios of regional warming levels for Cape Town regions (RWL), even though we only have simulation output for a single emissions pathway. We use this approach to compare different water management policies under different amounts of warming. The four levels of temperature change represent future climate scenarios from most severe to least severe. Under the ensemble of realizations, these scenarios correspond to different temporal intervals (Table 1).

The two-way coupling mechanism between the ABM and hydrologic model allows these models to exchange feedbacks at a monthly timestep (Fig. 1). Each month, the hydrologic model calculates the net inflow based on climate information and passes the current reservoir storage level (the volume of the available water) to the ABM. The ABM then simulates water managers using current water supply and demand conditions to determine the release to water, energy, and food sectors under each policy scenario. Finally, the ABM passes the water usage to the hydrologic model, which updates the reservoir level.

2.1. The agent-based model

The agent-based model consists of 3 sub-models: the agricultural model for vineyard irrigation and other irrigation demand, a hydropower generation model for the Steenbras upper dam, and the urban water usage model of citizens and other institutional water users including businesses and industries in the city of Cape Town.

For the agricultural sector, our model considers the agricultural activities in the wine regions adjacent to Cape Town. Within the scope of this paper, we only model the irrigation demand of viticulture in Cape Town because vineyards represent the most economically important and water intensive component of the agricultural sector in the region. For simplicity, we assume that water consumption from other crops is proportional to vineyard use, and thus represents a consistent fraction (57%) of the total irrigation demand. The agricultural sub-model was adopted from the original model and is described in detail in the model Overview, Design concepts, and Details (ODD) document (<https://github.com/ding-k/Cape-Town-ABM>) (Ding et al., 2019).

For the energy sector, we model the Steenbras hydropower dam with 180 MW of generation capacity. We assume the dam can fully operate when the total storage level of the water supply system (total storage level hereafter) is more than 20% of its maximum. When the total storage level is less than 20%, we assume the Steenbras dams cannot be kept at full anymore and a linear decrease in hydropower generation, and the hydropower generation capacity decreases to zero as the total storage level falls below 15% of its maximum. The energy sub-model is also adopted from the original model and is described in detail in the ODD (<https://github.com/ding-k/Cape-Town-ABM>) (Ding et al., 2019).

The urban water usage sub-model includes agents representing households and institutional water users, such as businesses and industries, in each of 94 wards. We model each of 94 wards as a single agent, which represents all the households and institutional water users in that ward. Each agent is characterized by parameters corresponding

Table 2

Scale, cost, and energy consumption of different water supply sources.

Water Supply Sources	Scale of Augmentation (Million Liters/Day)	Construction/Operational Cost (Rand/kL)	Energy consumption (kWh/kL)
Surface water	60	5	-
Groundwater	100	6	-
Wastewater reuse	70	7.5	2
Desalination	120	36	4

to the number of households, the average household size, the average unrestricted water demand for households and institutional users, the median annual household income, and the price elasticity of water demand for the median household. The heterogeneity of household income is reflected at the ward level, and the households within a ward are treated as homogenous because household-level microdata is not available. Future work will explore the effects of intra-ward heterogeneity.

We assigned values for these parameters based on data from the local and national demographic survey ([Cape Town Department of Water & Sanitation, 2018](#)). For the initial average water demand of the households and institutional water users, we use the water usage data of 400 residential regions in Cape town in 2013-a pre-drought normal year ([Cape Town Department of Water & Sanitation, 2018](#)). For the number, size, and income level of households, we use the demographic data from the 2011 census survey at the ward level. To overcome the challenge of the difference in spatial scales of the water usage and sociodemographic data, we aggregated the usage data to the ward level. The sub-ward residential regions do not always fall in a single ward. Where a residential region spanned multiple wards, we assigned it to the ward that contained the largest portion of its area. Cape Town comprises 1.12 million households, with an average of 3.4 people. After the aggregation, the 94 wards accounted for the entire population (22 wards had no residential regions assigned to them). Residential consumption accounts for 70% of urban water use ([Cape Town Department of Water & Sanitation, 2018](#)). We calibrated the initial water demand in the household and institutional sectors to match this ratio. We assign each of the 94 wards to one of four income levels based on its median annual household income: 30,000, 57,500, 117,000, and 230,000 as the income above 200,000 (200k), rand per year per household. These levels represent a roughly exponential sequence where each level represents roughly twice the income of the previous one. We represent each ward by an aggregate price elasticity based on the ward's median income level. It is widely observed that households with greater income are less sensitive to prices, so we assign greater price elasticities to lower-income wards. For a general price elasticity ϵ_D , we assign an income-dependent elasticity $\epsilon'_D = \epsilon_D - 0.3$, $\epsilon_D - 0.2$, ϵ_D , and $\epsilon_D + 0.3$, for the four income levels, from low to high. We assign each ward a price elasticity drawn at random from a normal distribution with a mean of ϵ'_D and a standard deviation of 0.05. We assign institutional and agricultural water users the general price elasticity ϵ_D . We also design additional sensitivity analysis for the price elasticity of agricultural water users in which we vary the ϵ_D from -0.3 to -0.7 at 0.1 interval and compare the reduction level of water usage for the agricultural sector and the dam storage with the baseline where the ϵ_D of agricultural water users is the general price elasticity.

2.2. The hydrologic model

All the water in our model is supplied by the “Big Six” reservoir system that supplies Cape Town and other regions of Western Cape Province. We simulate the water supply using the “Big Six” hydrologic model, a water balance model developed for this system and used by water managers there ([Climate System Analysis Group, n.d.](#)). This model was officially used to monitor and manage water resources during the Day-Zero crisis. The hydrological model apportions rainfall into runoff

and infiltration and accounts for evaporation of soil moisture as a function of potential evapotranspiration and the level of saturation (soil moisture content/available water content). The model is calibrated and has been validated by comparing simulation results to historical observations during the period from 2008 to 2018. Complete descriptions of the big six model are documented on the product website (<http://cip.csag.uct.ac.za/monitoring/bigsix.html>).

2.3. Data

The ABM and the “Big Six” model were calibrated using the historical climate and reservoir data from 2009 to 2018. We adopted the parameters for the agricultural, energy, and municipal sectors from the earlier version of the model ([Ding, Gilligan, et al., 2019](#)).

The primary climatic inputs were precipitation and potential evapotranspiration for the hydrologic model and monthly soil moisture deficit, which the agent-based model used to calculate the irrigation demand. The potential evapotranspiration is calculated as an average value across the Breede and Berg sectors that represent the “Big Six” catchment ([Fig. 1](#)). The precipitation is taken as the average of meteorological stations located at five of the “Big Six” reservoirs. We use linear regression to calibrate the average PET against the historical data from 2009 to 2018. We calculated the soil moisture deficit in each of the wine regions under each of the four downscaled climate models by applying Jacobi et al's (2013) PDSI tool to the gridded temperature and precipitation model output fields.

2.3.1. Precipitation and potential evapotranspiration under climate scenarios

The two key input variables of the “Big Six” model are monthly potential evapotranspiration (PET) and precipitation (PR). For historical data, these are composite values from multiple weather stations and under climate simulations, these are taken from gridded model output fields. The composite PET input used in the original “Big Six” model from 2009 to 2018 was a single time series of Penman-Monteith ET₀, representing the arithmetic average of the individual values of ET₀ at the 35 meteorological stations in the Breede and Berg sectors of the “Big Six” catchment ([Fig. 1](#)). We prepared the PET input for the model runs from 2009 to 2100 by applying a similar procedure to the gridded downscaled model output for the four downscaled climate models. These downscaled models had relatively coarse spatial resolution (0.44° by 0.44°) compared to the density of observational stations: the Breede and Berg sector contains 35 stations and is covered by 13 grid cells. Therefore, for the model runs from 2009 to 2100 we calculated average PET as the average of the PET values for each grid cell in the sector. Over the period 2009 to 2018 the calculated composite PET for all four members of the ensemble was lower than the historical composite PET calculated from observational data. We used linear regression to adjust the PET for the climate scenarios to match the calculated values over this period ([Fig. 2](#)).

Unlike PET, the downscaled simulated precipitation values for the first decade of the simulation period were in the same range as the composite observational value used in the original “Big Six” model from observations at the reservoirs so no adjustments were required. Overall, the climate projections from the four climate scenarios show a decline in rainfall and an increase in potential evapotranspiration.

3. Policy design

Policy 1, which we use to test hypothesis H1, is adapted from [Ding et al. \(2019\)](#). It takes a simple adaptive approach that reduces the water demand when the reservoirs show early signs of drought. This policy allocates water to meet the full demand of water users from municipal and agricultural sectors as long as the seasonally adjusted storage level of the reservoirs is above a threshold, which we specify as a fraction of the long-term average storage level (Algorithm 1). When the storage

level falls below the threshold, the policy raises the price of water to reduce demand.

Algorithm 1 Allocations for Policy 1 and 2

```

if  $V > 0.9V_{max}$  then
    Allocate full water demand to each sector // No restriction
else
    Calculate desired change in urban consumption:  $\% \Delta D = \frac{V_{avg} - V_{current}}{V_{avg}}$  // Level 2
    restriction
    Assign water tariff (new price) based on the price elasticity of demand ( $\epsilon_D$ ) // Urban sub-model
    Calculate actual water usage of households in 94 wards based on their price elasticities of demand ( $\epsilon_{Dj}$ ) // Urban sub-model
    Calculate reduced allocation to the agricultural and other institutional water users
    Calculate the average water bill for households in 94 wards // Urban sub-model
    Allocate water
end if

```

Note: V_{avg} and $V_{current}$ are the long-term average and current reservoir storage level of the month.

The price-elasticity of demand ϵ_d is defined as

$$\epsilon_d = \frac{dQ}{dP} \quad (1)$$

where Q is the consumption and P is the price.

The new price P_1 to achieve a reduced demand (Q_1) are calculated from the previous price and consumption (P_0 and Q_0) by integrating Equation using the unmodified basic price-elasticity ϵ_d (Equation 2).

$$P_1 = P_0 * \left(\frac{Q_1}{Q_0} \right)^{\frac{1}{\epsilon_d}} \quad (2)$$

We then calculate the individual consumption Q_{1i} of each ward i using that ward's price elasticity ϵ_d (Equation 3).

$$Q_{1i} = Q_{0i} * \left(\frac{P_1}{P_0} \right)^{\epsilon_{Di}} \quad (3)$$

Cape Town suffers from great income inequality, with a Gini coefficient for income of 0.6 and a poverty rate of 19% (Karuri-Sabina 2016; Sieff 2018). The tariffs imposed by Policy 1 may impose hardship on low-income households, and indeed the tariffs imposed in 2017-2018 left lower income households struggling to afford water while wealthy households continued to fill their swimming pools (Sieff 2018). Avoiding these disparate outcomes motivates Policy 2, which augments Policy 1 by providing a basic level of necessary consumption free of charge. Following current South African policy (Cape Town Department of Water and Sanitation, 2018), it provides up to 6 thousand liters (kL) of free water for households with annual incomes below 30,000 Rand. These households pay for any consumption beyond 6 kL at the same price as others.

The key parameter in Policy 1 and 2 is the general price elasticity of demand for water, which is used to adjust the tariff when reservoir levels are low. The elasticity is negative, meaning that demand drops as prices rise, and larger magnitudes correspond to greater sensitivity to price. We conducted sensitivity analysis to elasticity by running simulations of Policies 1 and 2 for three values of ϵ_D : -0.4, -0.5, and -0.6.

Cape Town is considering policies to augment its current water supply by adding additional surface water impoundment at Voelvlei reservoir, groundwater extraction with recharge at Cape Flat and Table Mountain aquifers, wastewater reuse, and desalination (Cape

Town Department of Water & Sanitation, 2018). Policy 3 explores the implications of this water augmentation plan and quantifies the energy tradeoff by energy-intensive water supply sources such as desalination and wastewater reuse. This policy examines the sufficiency and reliability of these 4 different water supply sources. We adapt the estimation of construction cost and energy consumption (only for wastewater reuse and desalination) to calculate the new water price (Table 2).

In calculating the new water price with water augmentation, we account for both the operational cost of existing surface water sources and the cost of the new water supply. We assume that the cost of surface water from the augmented impoundment at Voelvlei will be the same as the cost for water from the existing surface water storage: 5 R/kL. The total cost for the augmented Cape Town water, C_{new} , is calculated as

$$C_{new} = \frac{C_{sw} * V_{sw} + C_{nsw} * V_{nsw} + C_{gw} * V_{gw} + C_{gwr} * V_{gwr} + C_{ds} * V_{ds}}{V_{new}} \quad (4)$$

where C represents the cost, V represents the volume, sw and nsw denote existing and added surface water, gw denotes groundwater, wwr denotes wastewater reuse, and ds denotes desalination.

Augmentation alone will not solve the water shortage. A new normal reduction (NR) in water use, a universal demand reduction for all Capetonians moving beyond the "Day-Zero" crisis proposed by the city government, is needed for the water supply to be sustainable even with augmentation. To test the sustainability of the augmented water supply system, we ran simulations for a range of NR from 0 to 45% in 5% increments under each of the four climate scenarios, as realized by each of the four downscaled models.

4. Results

We ran the model in configurations specific to the 3 policies from 2009 to 2100 driven by climate output from each of the four downscaled models (Fig. 2) and then extracted 30-year intervals from each model run corresponding to the four different warming scenarios in which the mean global temperature during the interval is 1.5°C, 2.0°C, 2.5°C, and 3.0°C above pre-industrial temperatures. It is important to note that we do not posit that policies will remain the same over a century, but we use the long simulation runs to generate the 30-year intervals that will be used to assess the performance of each of the three water management policies under different amounts of warming. We organized our model outputs into 48 sets, corresponding to each of three policies, under four different amounts of warming, as realized by each of four different climate models. We assessed the FEW system outcomes using overall dam storage, reduction of water consumption, water affordability, and hydropower generation.

4.1. Overall dam storage

It is critical to maintain reservoir storage levels in the "Big Six" system above 20% of total storage capacity because when storage drops below this threshold, hydropower generation capacity declines and it becomes harder to extract water from the reservoirs.

Under Policy 1 and 2, the dam storage can be maintained above the 20% threshold even at 3°C global warming level (GWL) under all four climate models except the model with the highest climate sensitivity (M1). The dam storage levels for policy 1 and policy 2 were close, but with slightly lower levels of Policy 2 because of free water supplied to the indigent households (Fig. 3). The dam storage levels were relatively insensitive to the general water price elasticity, which is to be expected because the elasticity is used within the policy model to set tariffs. We

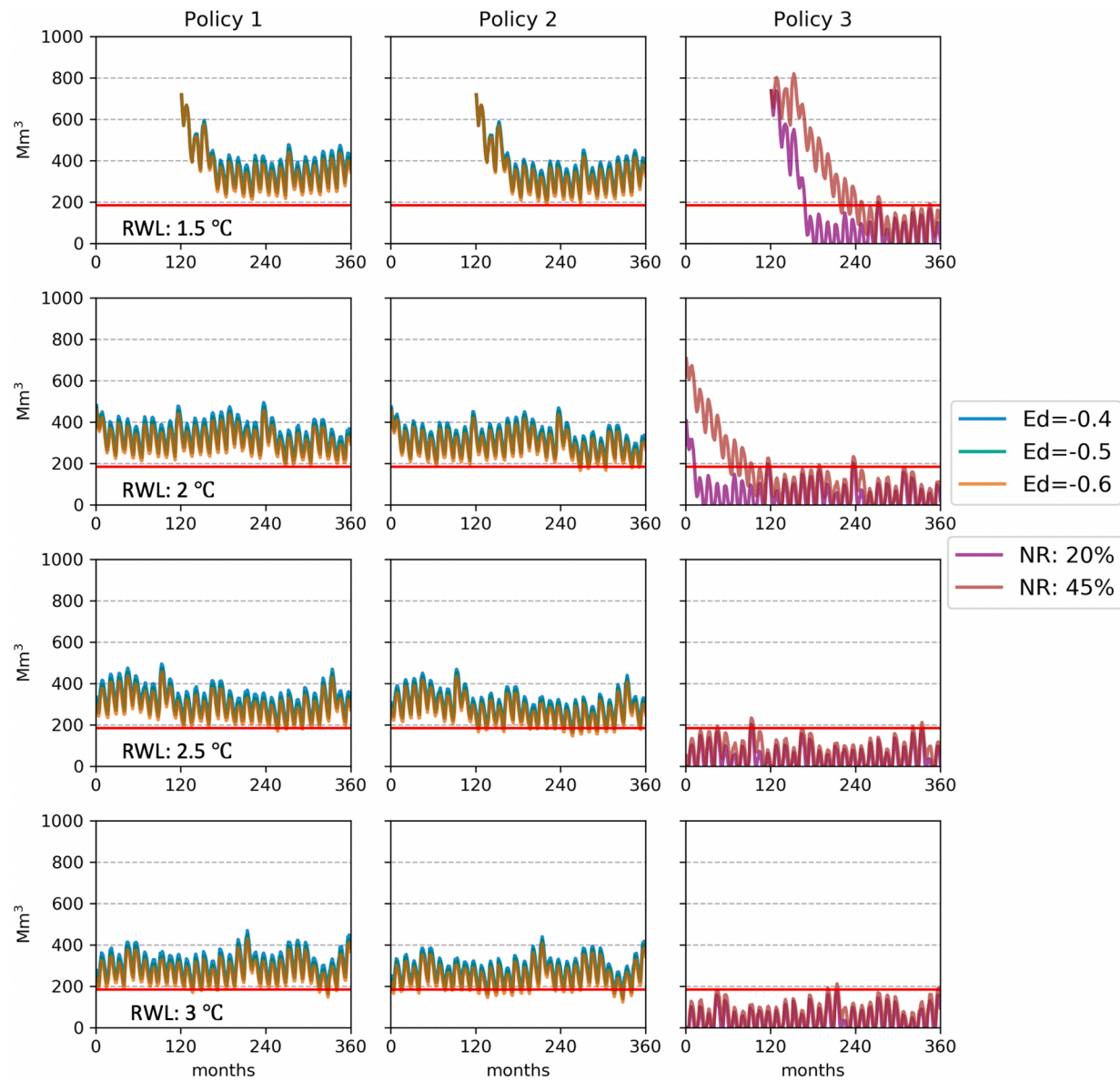


Fig. 3. overall storage for Policy 1, 2, and 3 (columns from left to right) for the 30-year periods of 4 climate scenarios 1.5°C , 2°C , 2.5°C , and 3°C (rows from up to bottom) of warming as realized by Climate Model M1. The red line indicates the critical threshold of 20% of the maximum storage capacity. Ed represents the general price elasticity of water demand, and NR represents the level of new normal reduction.

Table 3
summary of average water usage reduction of households at different income levels.

Climate/Policy Scenarios		30k Rand/month	57k Rand/month	117k Rand/month and agricultural sector	200k Rand/month
CS1	Policy 1	Constantly under intense reduction, cut to less than 10% of the original demand (OD) towards higher global warming levels (GWLS).	Constantly under intense reduction, cut to less than 20% OD towards higher GWLS.	Constantly under serious reduction, cut to less than 35% OD towards higher GWLS.	Under moderate reduction, cut to no more than 60% OD in the worst conditions.
	Policy 2	Constantly fluctuate between 50% and 70% OD	Similar but slightly worse than P1.		Similar to P1.
CS2/ 3/4	Policy 1	Frequently under serious reduction, cut up to 30% OD in higher GWLS.	Frequently under serious reduction, cut up to less than 40% OD in the worst conditions.	Frequently under moderate to serious reduction, cut up to 50% OD in worst conditions.	Under minor to moderate reduction, cut to less than 80% in the worst conditions.
	Policy 2	Under large fluctuations ranging from half to full demand.	Similar but slightly worse than P1.		Similar to P1.

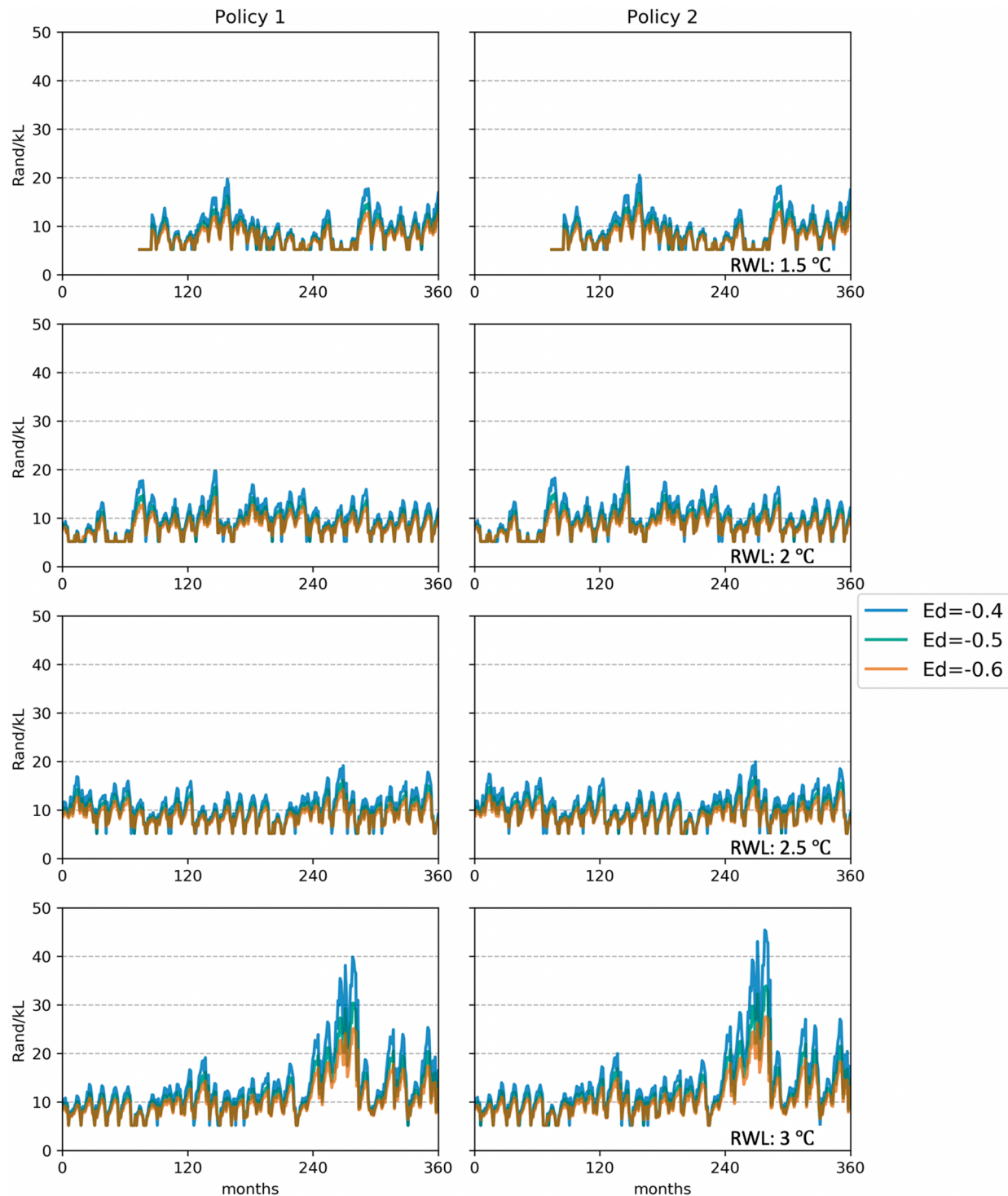


Fig. 4. water prices for Policy 1, 2, and 3 (columns from left to right) for the 30-year periods of 4 climate scenarios 1.5°C, 2°C, 2.5°C, and 3°C (rows from up to bottom) of warming under Model 2 in the ensemble. Ed represents the general price elasticity of water demand.

did additional sensitivity analysis for the water price elasticities of the vineyard farmers for all climate scenarios, and it also did not make significant impact on the reservoir storage (examples shown in Figs. A7 and A8). Under all climate scenarios, the dam storage levels trended downward at higher GWLs (M1, 2, 3, and 4 shown in Figs. 3, A1, A2, and A3, respectively).

Under Policy 3, the government-proposed new normal reduction rate of 20% was only sufficient to manage the storage level above the threshold of 20% of the total storage capacity for climate model M3, which had the most rainfall for each level of warming, while for models M2 and M4, new normal reduction rates of 45% or higher are needed to maintain achieve a similar storage levels (Figs. 3, A1, A2, and A3).

Model M1, with the greatest climate sensitivity, the reservoirs struggled to avoid complete depletion despite the water augmentation and new normal reductions of 45% under the more extreme climate scenarios (Fig. 3).

4.2. Water use reduction of different agents from FEW sectors

The first two policies use demand-side management with variable water tariffs to achieve the resources conservation target and assure water supply to users across the FEW sectors. Policy 3 augments the water supply to achieve the same goal as the previous two policies, but with smaller reduction of demand.

Policy 3 applies a uniform reduction of consumption across all sectors through command and control regulation, whereas Policies 1 and 2 implement flexible demand reduction that varies across sectors and across income levels within the household sector (Table 3). In policy 1, households with higher incomes experienced milder reduction of their water consumption than less affluent households, and the reduction rates decreased nonlinearly with increasing income levels of households in all climate scenarios (Table 3). The households of more than 200k Rand/year cut their usage to about 60% of their original demand at most, while other households used 10% to 30% of original demand under the 3°C warming scenario. In policy 2, the free allocation of basic water to indigent households reduced this disparity: middle-income households experienced slightly more water usage reductions, although the wealthiest households did not reduce their consumption much more than under policy 1 (Table 3). Across all scenarios and models, High income households did not respond nearly as much as lower or middle income households to tariff increases.

Under policies 1 and 2, households at different income levels were moderately sensitive to general price elasticities. The gap in reduction rates between the highest (-0.4) and lowest (-0.6) general price elasticities further expanded as climate scenarios became more severe. Higher general price elasticities resulted in higher price tariffs (Fig. 4), and the reduction levels are consequently higher across the FEW sectors.

The reduction rates for the agricultural sector and other institutional urban water users varied across the three policies. In policy 1 and 2, the water usage reductions in the agricultural sector and the other urban sector were the same as the reduction rates of households with 117 k Rand per year (Table 3), because their price elasticities were assumed to be the same as the general price elasticity. Compared to Policy 1, the agricultural and other urban users experienced slightly more reduction as a trade-off to the free basic water policy under Policy 2 (Figs. A9 and A10). In Policy 3, the water reduction rates were the same across all water users as the reduction rates depend on the decision of the final new normal rate made by the policymakers.

4.3. Water affordability

Water availability determines the water price in Policy 1 and 2 because the reduction target of water usage is realized by the price tariff. Under the realization by climate model M1, the unit price of water could go above 100 and 180 Rand per thousand liters in Policy 1 and 2, respectively, at 3 °C RWL (Fig. A4). While under realizations by climate models M2, 3, and 4, the unit water price ranged from 5.2 to 40, and from 5.2 to 50 Rand/kL in Policy 1 and 2, respectively (Figs. 4, A5, and A6). Compared to Policy 1 and 2, the water price of Policy 3 was more affordable because it does not rely on price but used a uniform command-and-control restriction of water usage. The calculated water price after factoring in the costs of all types of water augmentation was about 8 Rand/kL.

Because households at different income levels have different individual price elasticities, their monthly water bills vary significantly in the first two policies. The indigent households could only afford to pay

about 100 Rand per month for water, while households for income levels at 57k, 117k, and 200k Rand per year could pay up to 200, 600, and 1500 per month for water. Policy 2 was designed to address the water affordability issue by offering free basic water to the indigent households, but the water bills for other households were consequently higher.

4.4. Energy generation and consumption

The hydropower generation capacity would be interrupted once the storage level falls below the critical threshold of 20% of the total storage capacity. In general, the hydropower capacity would be impacted more frequently as the GWLs intensifies in all policies. For Policy 1, the hydropower was rarely interrupted until the GWLs went up to 2.5°C or higher. Compared to Policy 1, Policy 2 experienced more frequent interruptions in hydropower generation as a trade-off due to the free water policy (Fig. 3, A1, A2, and A3).

Whereas in Policy 3, the hydropower dam could barely operate under the most severe climate scenario (CS1), and all water users needed to adopt a new normal reduction rate of 45% to ensure the hydropower dam operated at full capacity with minimum interruptions in other climate scenarios (Figs. 3, A1, A2, A3). Unlike the first two policies, the desalination and wastewater reuse consume a significant amount of energy to treat water. The desalination requires between 17.5 MW and 20 MW of power input for its operation at 120 MLD, and the wastewater requires 5.8 MW for its operation at 70 MLD. The combined power input accounts for about 14% of the full hydropower generation capacity.

5. Discussion

Application of a simple adaptive policy (Policy 1) can provide sufficient water to users across multiple FEW sectors with moderate average water use reduction and price tariffs at or below 2.5°C under all climate scenario except the worst-case scenario, CS1. Even under the worst-case scenario, Policy 1 effectively maintained the Cape Town regions away from a “Day-Zero” crisis and ensured minimal interruption for hydropower generation. However, Policy 1 created inequality of access to water in which households with lower income levels had to cut their water use much more compared to wealthier households (Table 3). This has been a persistent issue for policies of using water tariffs to reduce demand, and the issue exacerbates inequality during water crises (Sieff, 2018).

The second policy, designed to help the indigent households during critical times, provides a basic allotment to indigent households of 6 kL per month free of charge. It produced a slight decrease in dam storage levels, a modest increase of reduction rates for other water users, and more interruptions of hydropower generation under all climate scenarios. Policy 2 protected the indigent households when future climate conditions worsened and water availability shrunk in Cape Town. The significant improvement for the indigent households comes at a cost, more rigorous reduction rates for the households with income levels in the middle (middle-class hereafter)- 57k and 117k Rand per year, but not the wealthiest households (Table 3). The two middle-class households experienced a further 10 % reduction on average compared to Policy 1, and they had to cut 80 to 90% of their water use under the worst climate scenario. The wealthiest households did have to pay a hefty water bill – up to 1500 Rand per month – to maintain high water use rates, but this did not cause them to reduce their consumption by as much as middle and low-income households. Policy 2 reduces the inequality between middle and low-income households, compared to policy 1, but at the cost of imposing additional stress on the middle class, and without causing the wealthiest households to reduce their consumption any more than under policy 1.

The water augmentation plan of an additional 350 MLD capacity in

Policy 3 cannot sustainably meet the need of the water users across the FEW sectors, and it did not show better performance compared to Policy 1 and 2. Under the highest-sensitivity climate model (M1), the reservoir quickly depleted to below the critical threshold of 20% percent of the maximum storage capacity even under the 1.5°C scenario and never rebounded. Under the other members of the ensemble, the government proposed new normal reduction rate of 20% was not sufficient; at least a 35% reduction is needed to keep the storage level above the critical threshold to prevent reservoir depletion and ensure hydropower generation for climate scenarios with $GWL \leq 2.5^{\circ}\text{C}$ (Fig. 3: Policy 3). The energy consumption from desalination and wastewater reuse at a combined scale of 190 MLD was significant, accounting for 14% of total hydropower generated at its full capacity. Desalination also faces the issue of water quality as the seawater near the shores of Cape Town contains high concentrations of chemical and microbial contaminants (Tafirenyika, 2018). The pollution from industries, pharmaceuticals, agricultural practices, informal settlements, and so on impose additional challenges in water recycling methods such as wastewater reuse and in using groundwater (Kretzmann, 2019). Although the estimated water price of Policy 3 was only 8 Rand per kL, this price is not likely to be realistic given the much larger scale of water augmentation needed that would drive the cost of infrastructure and energy consumption higher.

An important caveat is that this analysis was conducted with the population size at 2009 levels, 3.8 million. The modeling results indicate Cape Town will face intensifying water stress and variations as the global warming levels increase. The issue will only be exacerbated if Cape Town keeps growing in size. With the projection using an ensemble of four downscaled models realizing the four climate scenarios of 1.5C, 2.0C, 2.5C, and 3.0C warming, we argue that 3.8 million is the cap for the current Cape Town water supply system. The augmentation of 350 MLD did not provide much help because the capacity of the original surface water will be shrinking as the rainfall decreases with higher regional warming levels (Figs. 2, A11, A12) at the same time under climate change.

5.1. Limitations and future works

The future of shrinking water availability intensifies the competition for limited water among the agriculture, urban freshwater, and energy sectors. Under all three policies, the agriculture sector including the wine producers can expect to experience a 20% to 60 % reduction of their irrigation capacity, just as the households and other urban institutional water users who share the general water price elasticity, ϵ_d . This future will likely call for a shift in agriculture practices, which may be a reduction in the area irrigated or an improvement in irrigation efficiency. Under more extreme climate conditions, agriculture and hydropower will be significantly impacted because the urban water users have the highest priority. Future works could include an actual wine production model to study the feasibility of the wine production in Cape Town. The social consequences cannot be neglected because reducing irrigation water will impose a huge economic and impact and possibly undermine social stability, as seen in other parts of the world such as California in the United States (Walters, 2019).

The treatment of uncertainty in agent-based models of coupled human-natural systems is a 'grand challenge' (Elsawah et al., 2020). A thorough exploration of uncertainty is beyond the scope of this paper, although we note that uncertainty in socioeconomic factors can have a greater impact on outcomes from models than biophysical factors. For example, price elasticities and income level we used in this study are estimated values and from survey, the data itself contains large degrees of uncertainty. We take a first step in this paper by exploring the sensitivity of our results to price elasticity.

In this study, we ran a series of simulations with a frozen technology and population assumption to establish a baseline, a scenario in which

how climate change along could impact Cape Town. Future works could incorporate technological advancement and social-economic growth in intermediate-term planning cycles to study how to mitigate the pressure of population growth on the regional water supply system and the food and energy sector where water is also a critical input. Future works could also consider the potential human migration triggered by climate change and stringent policies of resources conservation and price tariffs.

6. Conclusion

Our regional analyses conducted at the city and surrounding region level illustrate the future availability and variability of the essential FEW resources specific to their own unique societal and environmental conditions. In this study, we used a coupled human-natural system modeling approach to project the future of water resources use across FEW sectors—the Capetonians, wine agriculture, and hydropower generation under moderate to severe impact of climate change. Among the three policies of resources management, we found that adaptive water conservation could effectively maintain the regional water supply system above the critical threshold of 20%- a level to ensure very basic functioning for all stakeholders. Imposing a variable price tariff could effectively cut the water usage, but it also creates inequality of access to water for households at lower income levels. A policy modification that provides free basic water for indigent households increases the burden on middle-income households and has little effect on upper-income households. Our analysis showed that Cape Town's water supply system might already be at its capacity to serve the current population, wine production, and hydropower generation, and that rigorous water conservation practices across FEW sectors is needed to compensate for the negative impact of climate change. The water augmentation plan, including wastewater reuse and desalination in the government's proposal in 2018, may not be enough for the worst climate scenario, and also requires intensive economic and energy input to treat water. We conclude that future climatic stress on Cape Town will create difficult tradeoffs to address the disparate impacts of water scarcity upon different economic sectors in the FEW nexus, and upon households at different income levels. Augmenting the water supply to include groundwater, wastewater reuse, and desalination may reduce the severity of these tradeoffs somewhat, but is unlikely to eliminate them. As Cape Town and other cities and regions contend with questions of unequal access to water, our coupled human-natural system model can be applied to other policy options and can be adapted to other cities and regions to assess their own potential FEW-related challenges and to help create effective policies of sustainable resources management to achieve FEW security.

CRediT

Ke Jack Ding, Jonathan Gilligan, George Hornberger, and Y.C. Ethan Yang contributed to the conceptualization of this project. Ke Jack Ding collected the data, constructed the model, ran the analysis, and drafted the manuscript, figures and tables. Piotr Wolski Provided original the Big-Six hydrologic model. All authors edited, revised and approved the manuscript.

Declaration of Competing Interest

None.

Appendix: Additional results from the model simulations

[Fig. A1-Fig. A12](#)

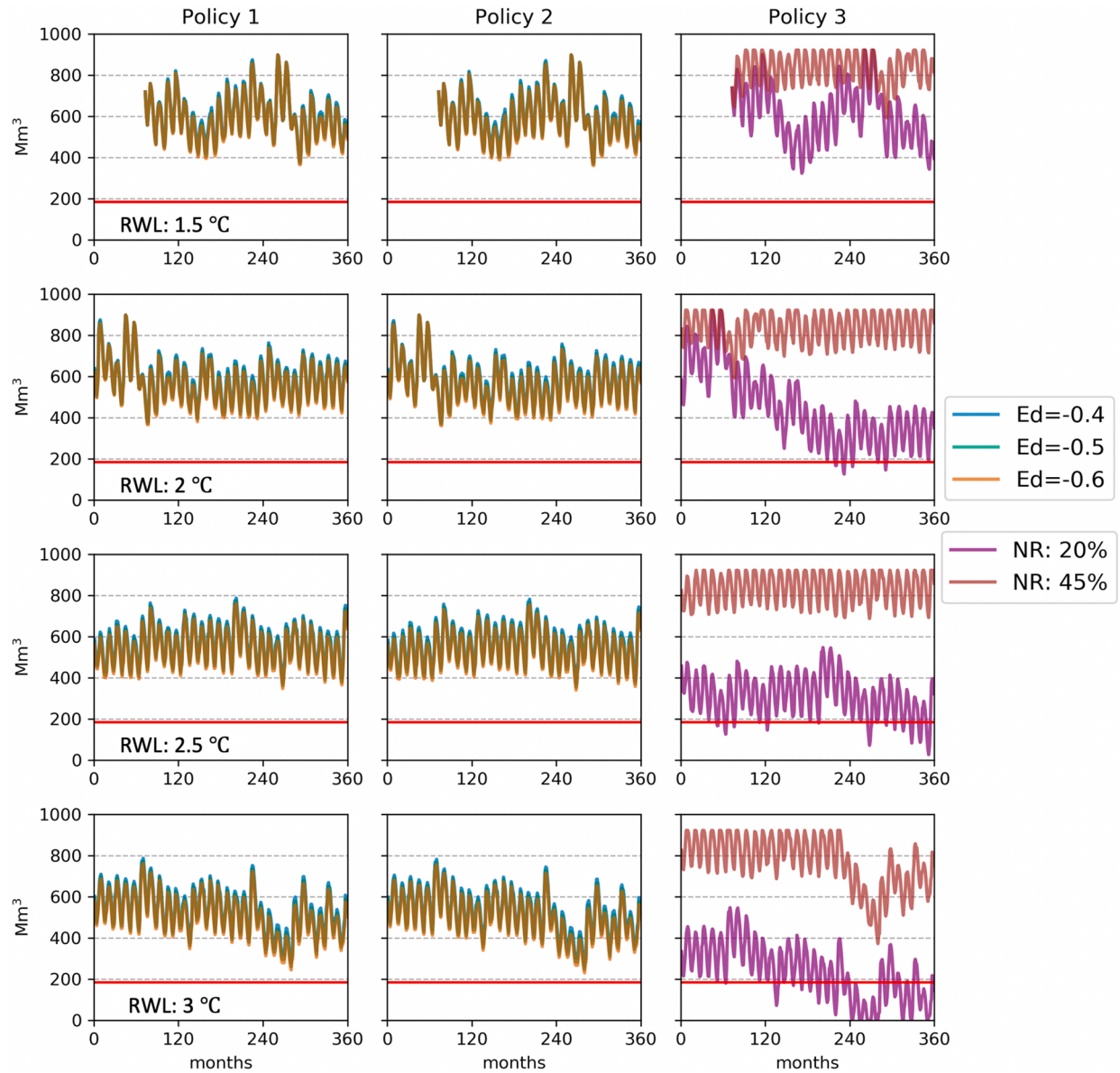


Fig. A1. overall storage for Policy 1, 2, and 3 (columns from left to right) for the 30-year periods of 4 climate scenarios 1.5°C , 2°C , 2.5°C , and 3°C (rows from up to bottom) of warming as realized by Climate Model M2. The red line indicates the critical threshold of 20% of the maximum storage capacity. Ed represents the general price elasticity of water demand, and NR represents the level of new normal reduction.

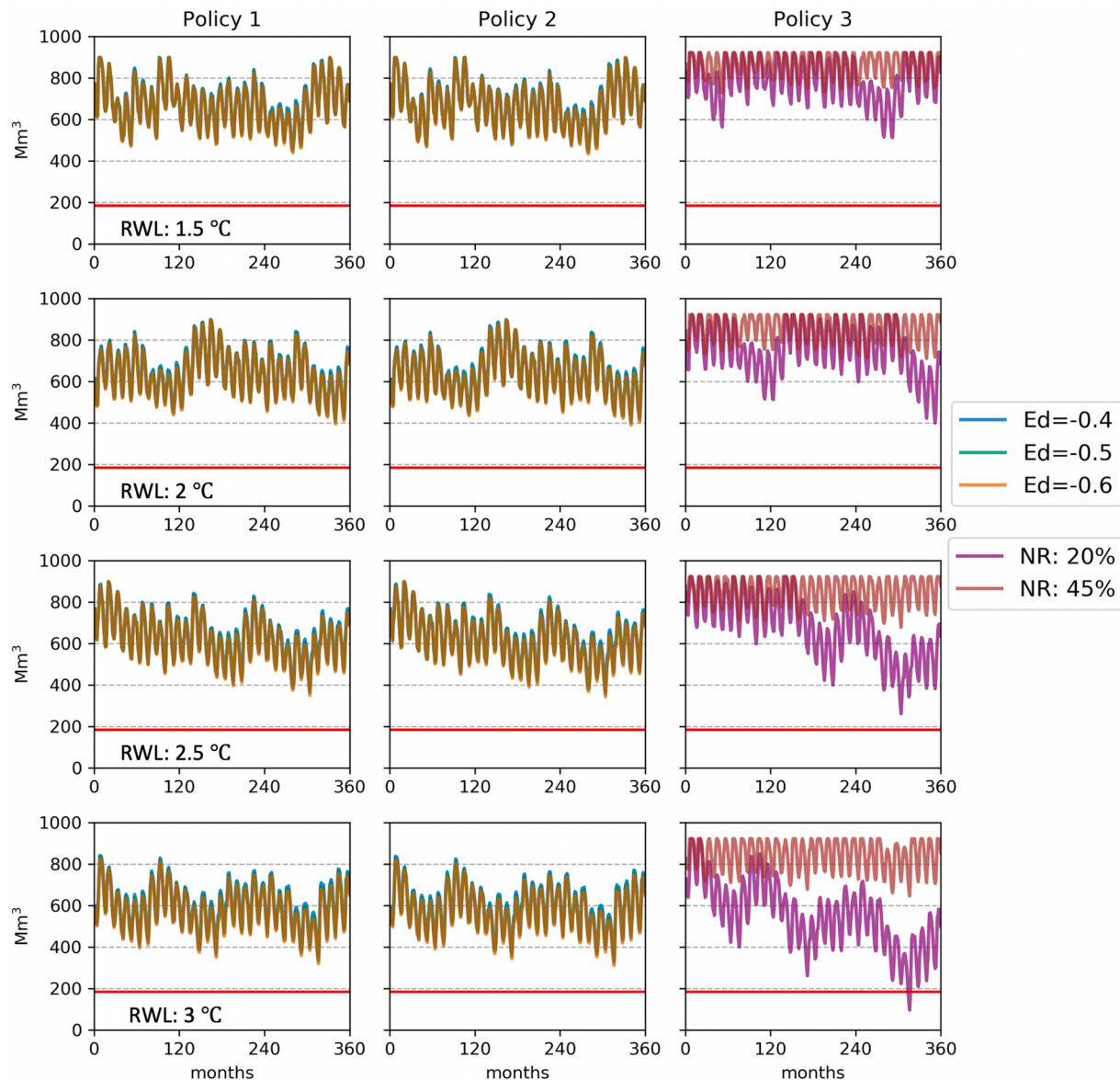


Fig. A2. overall storage for Policy 1, 2, and 3 (columns from left to right) for the 30-year periods of 4 climate scenarios 1.5°C , 2°C , 2.5°C , and 3°C (rows from up to bottom) of warming as realized by Climate Model M3. The red line indicates the critical threshold of 20% of the maximum storage capacity. Ed represents the general price elasticity of water demand, and NR represents the level of new normal reduction.

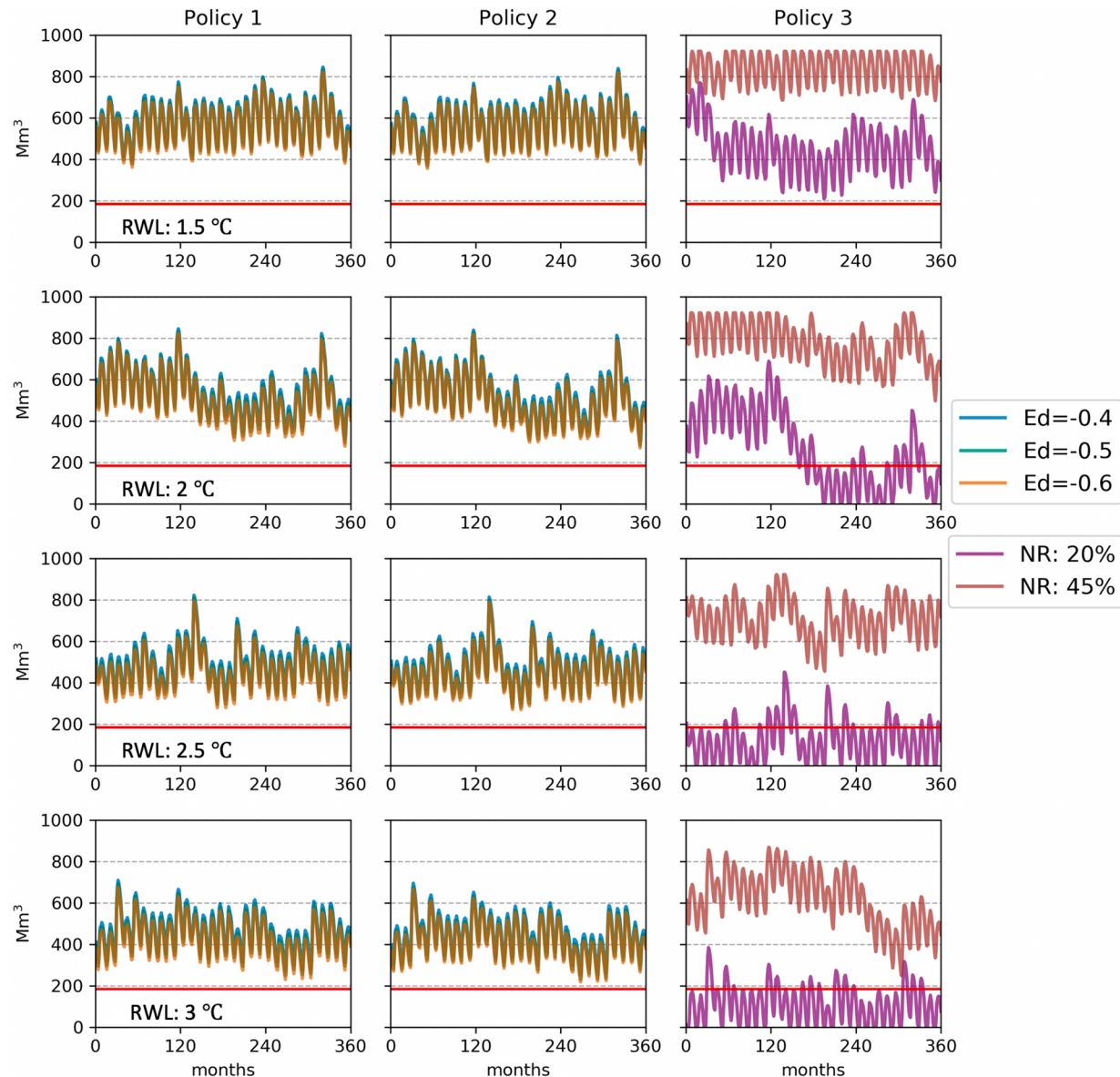


Fig. A3. overall storage for Policy 1, 2, and 3 (columns from left to right) for the 30-year periods of 4 climate scenarios 1.5°C , 2°C , 2.5°C , and 3°C (rows from up to bottom) of warming as realized by Climate Model M4. The red line indicates the critical threshold of 20% of the maximum storage capacity. Ed represents the general price elasticity of water demand, and NR represents the level of new normal reduction.

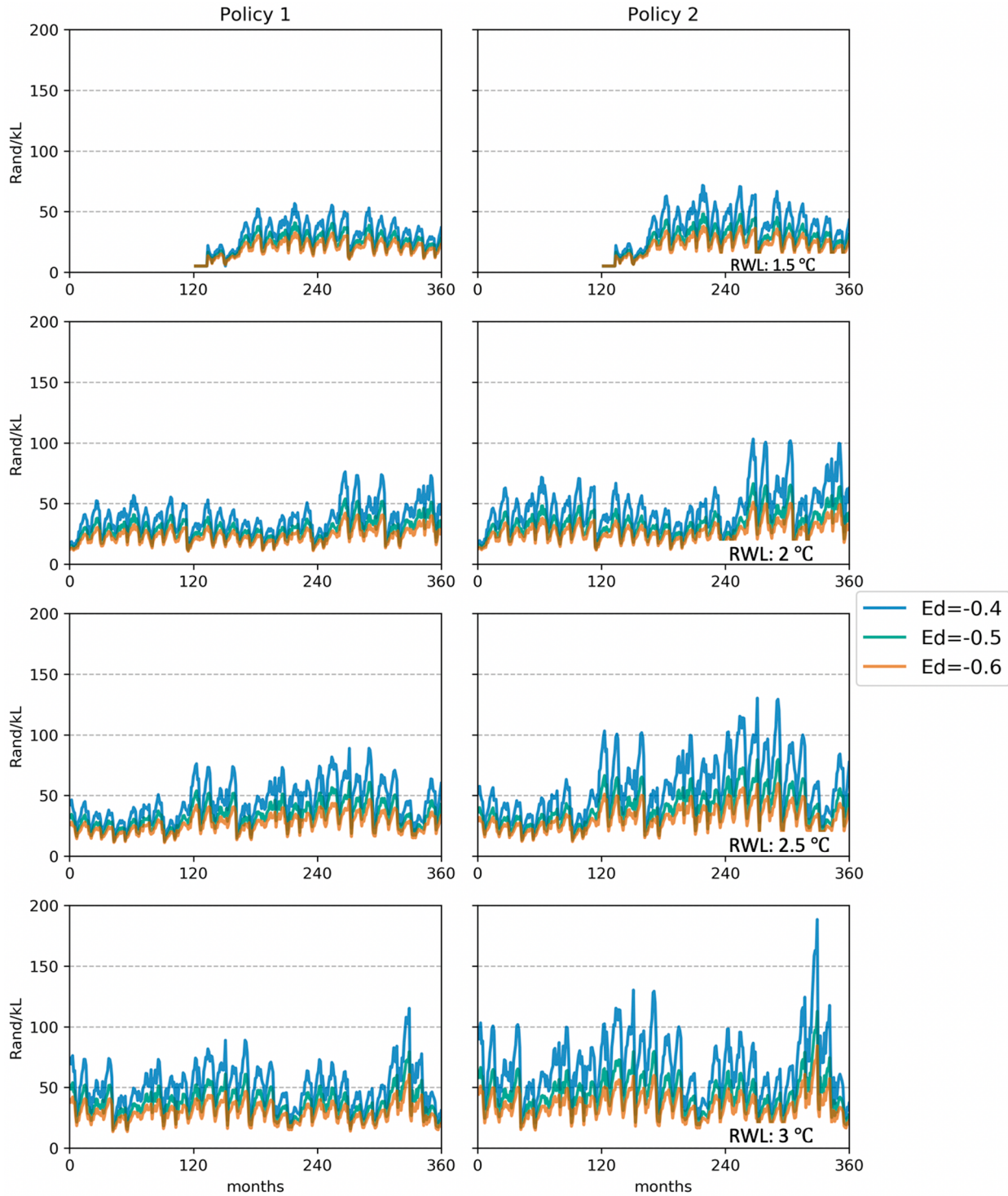


Fig. A4. water prices for Policy 1, 2, and 3 (columns from left to right) for the 30-year periods of 4 climate scenarios 1.5°C , 2°C , 2.5°C , and 3°C (rows from up to bottom) of warming as realized by Climate Model M1. Ed represents the general price elasticity of water demand.

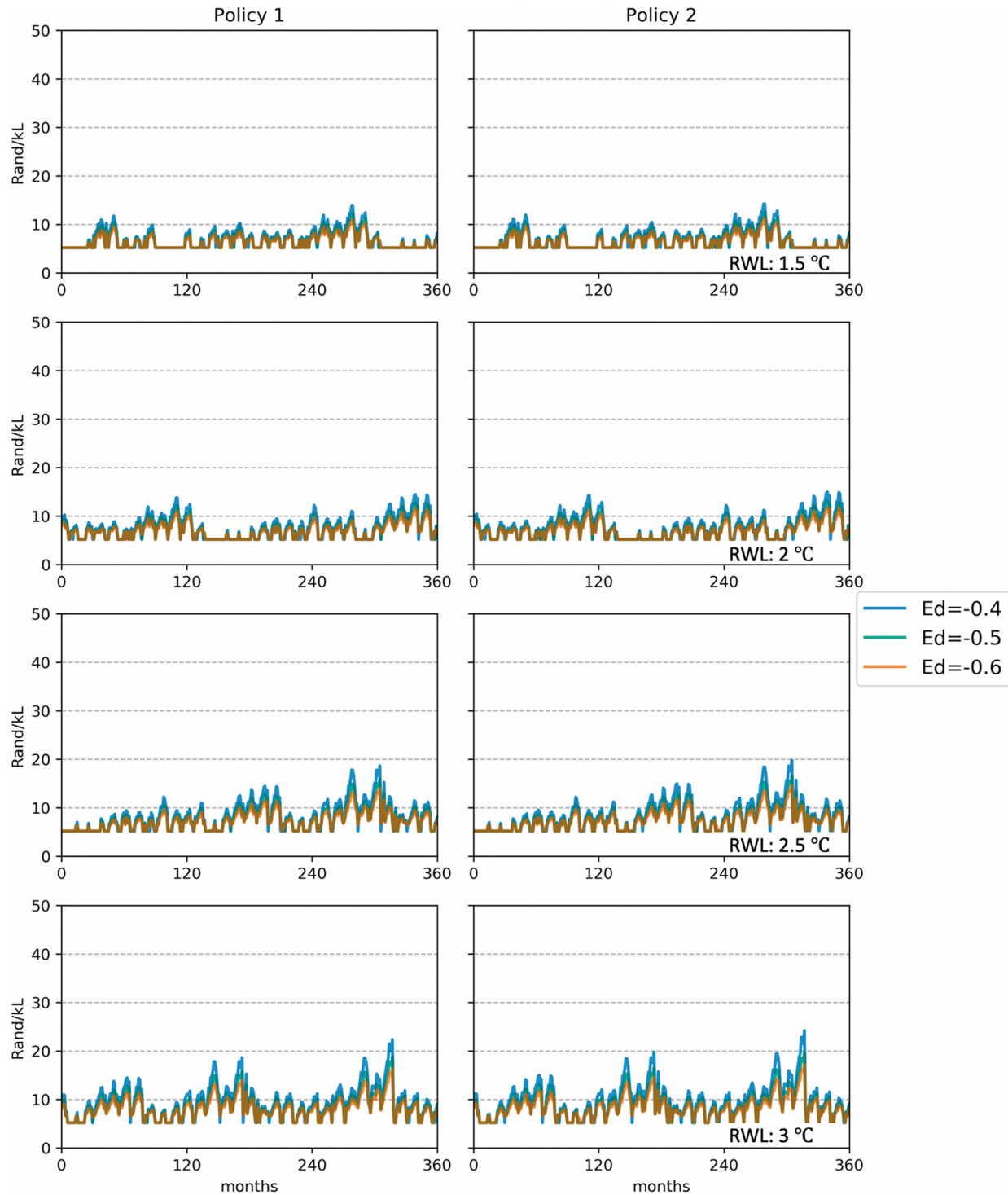


Fig. A5. water prices for Policy 1, 2, and 3 (columns from left to right) for the 30-year periods of 4 climate scenarios 1.5°C , 2°C , 2.5°C , and 3°C (rows from up to bottom) of warming as realized by Climate Model M3. Ed represents the general price elasticity of water demand.

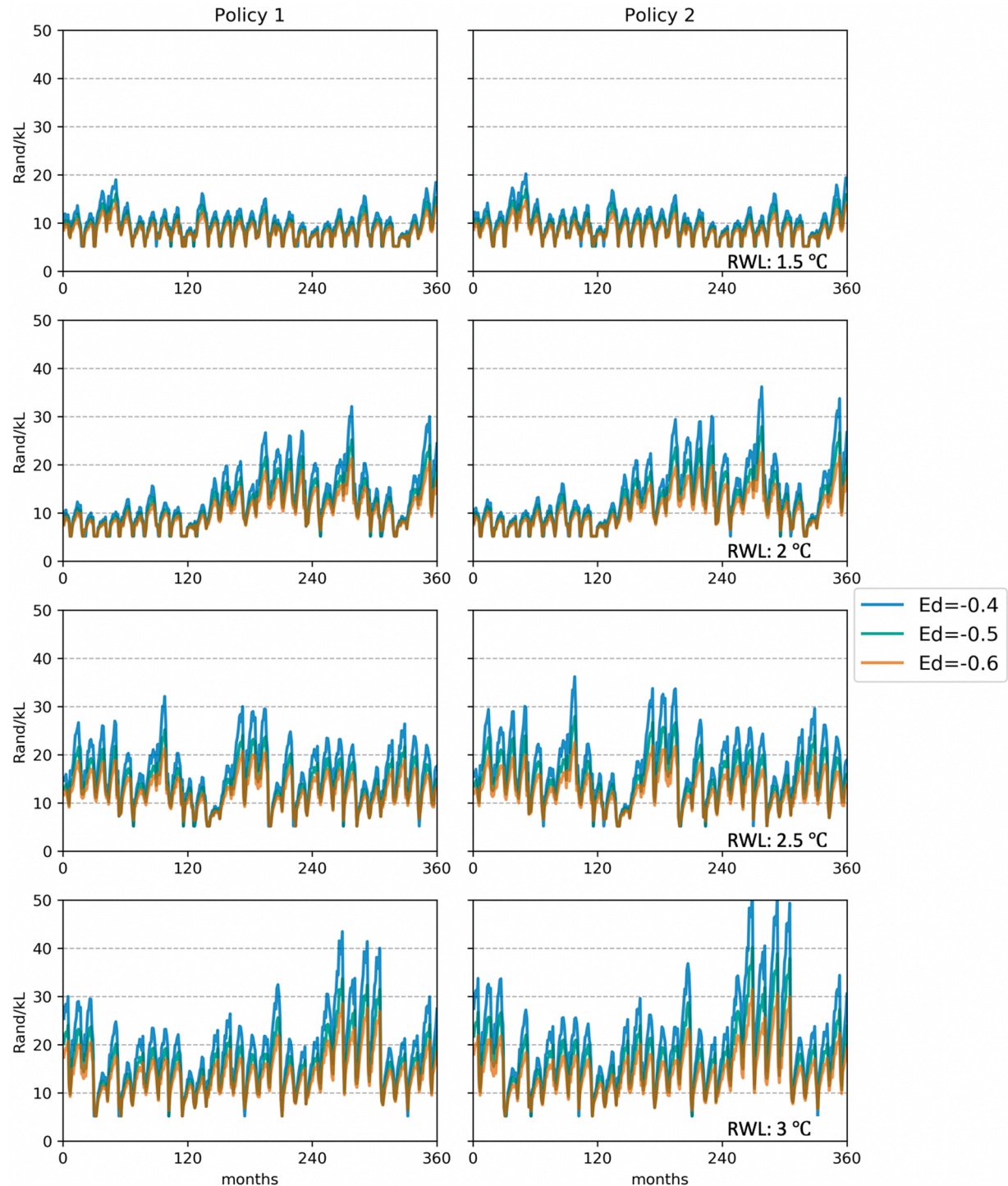


Fig. A6. water prices for Policy 1, 2, and 3 (columns from left to right) for the 30-year periods of 4 climate scenarios 1.5°C , 2°C , 2.5°C , and 3°C (rows from up to bottom) of warming as realized by Climate Model M4. Ed represents the general price elasticity of water demand.

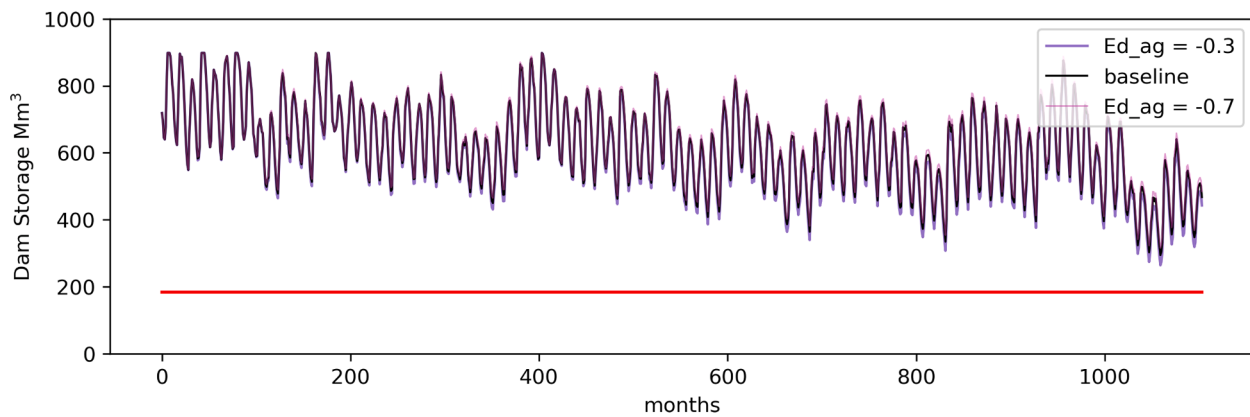


Fig. A7. Dam storage levels when changing price elasticities of water demand for vineyard farmers under Policy 1, Climate Scenario M3. The red line indicates the critical threshold of 20% of the maximum storage capacity.

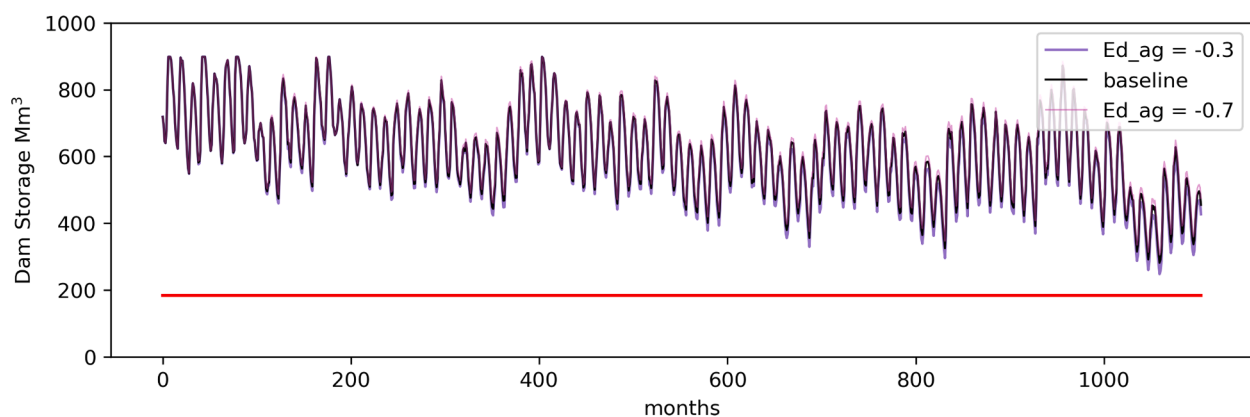


Fig. A8. dam storage levels when changing price elasticities of water demand for vineyard farmers under Policy 2, Climate Scenario M3. The red line indicates the critical threshold of 20% of the maximum storage capacity.

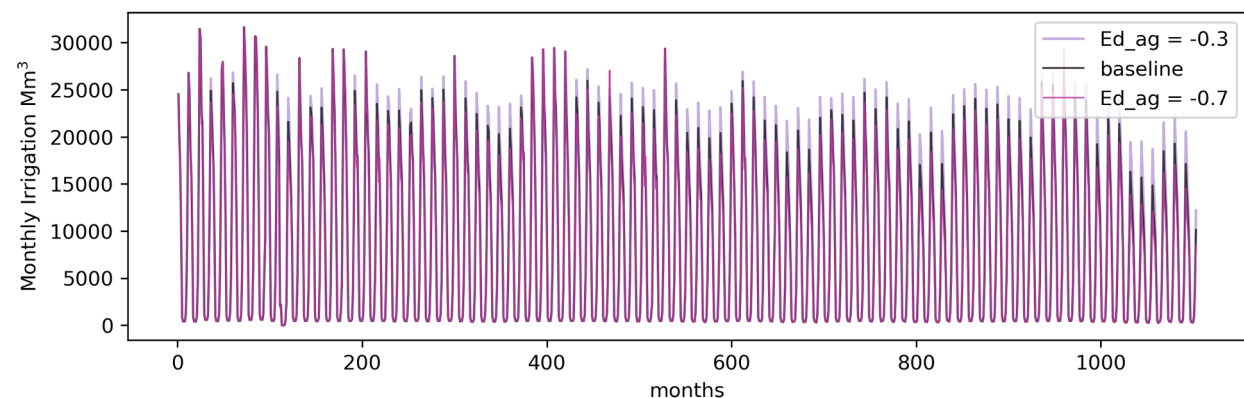


Fig. A9. reduction of vineyard irrigation under Policy 1, Climate Scenario M3. Baseline scenario is when price elasticity of water demand in the vineyards as same as the general price elasticity of water demand which is -0.5.

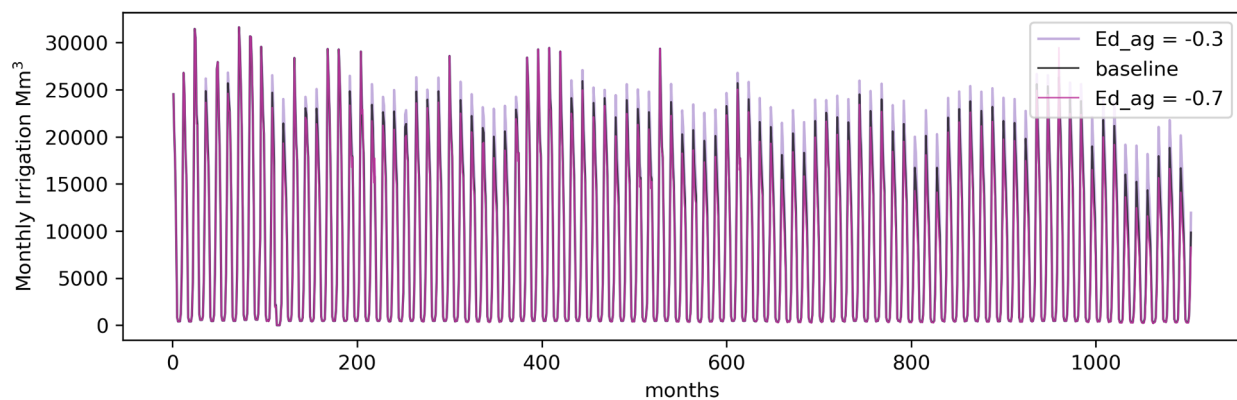


Fig. A10. reduction of vineyard irrigation under Policy 2, Climate Scenario M3. Baseline scenario is when price elasticity of water demand in the vineyards as same as the general price elasticity of water demand which is -0.5.

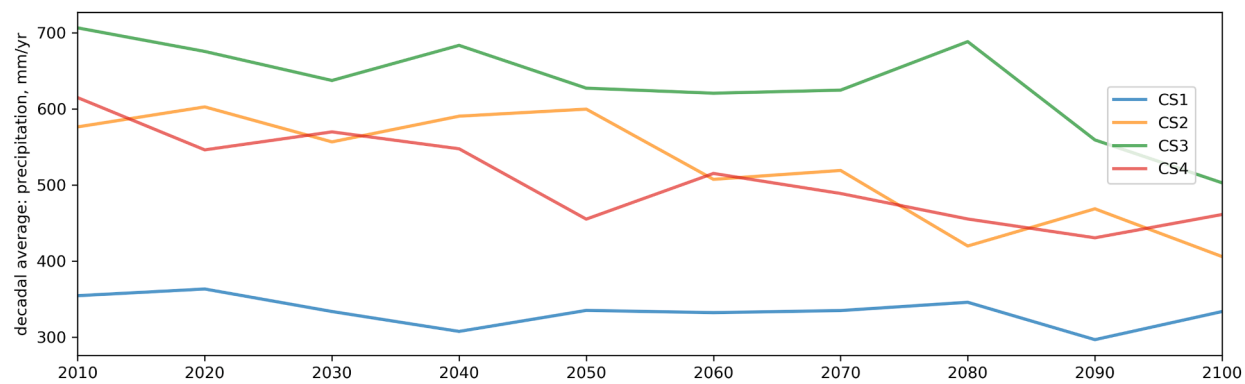


Fig. A11. decadal average of precipitation in the study region. The four lines, CS1, 2, 3 and 4 correspond to the precipitation in four climate scenarios generated by model M1-M4 we used in this study.

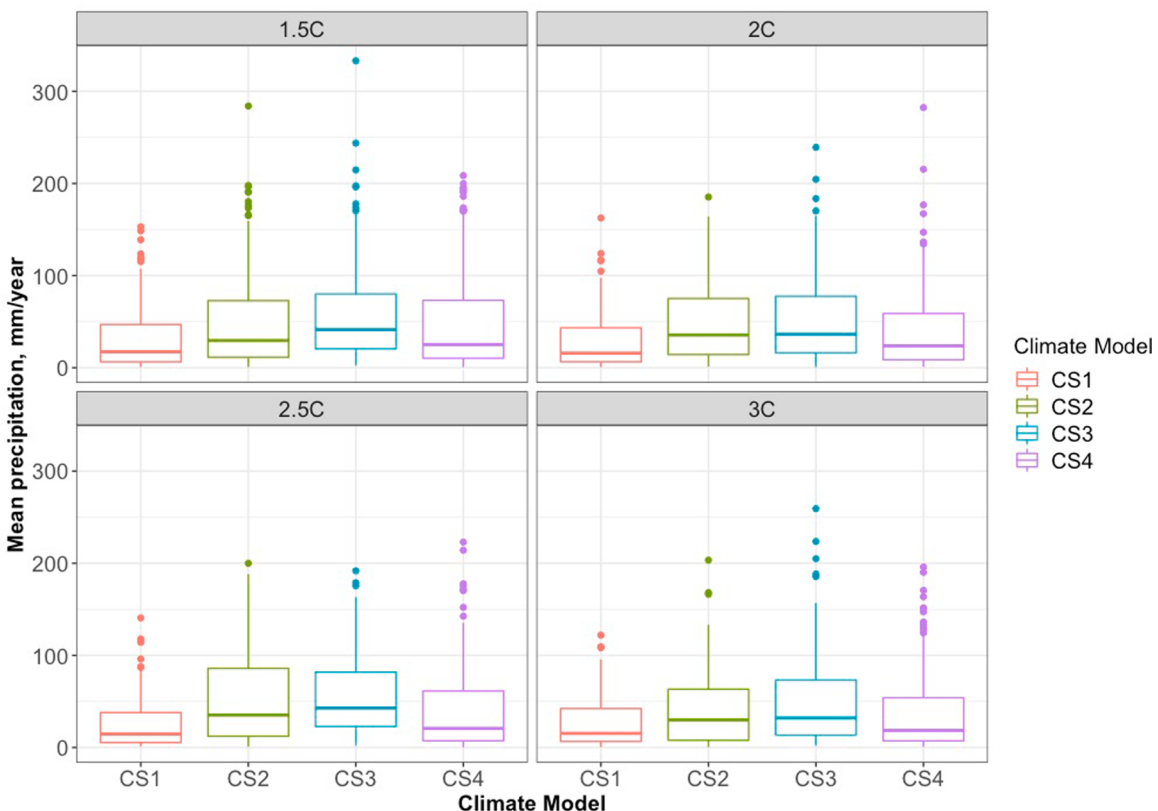


Fig. A12. boxplot of mean precipitation in different during different periods of regional warming levels. CS1, 2, 3 and 4 correspond to the precipitation in four climate scenarios generated by model M1-M4 we used in this study.

Reference

- Allen, M.R., Frame, D.J., Huntingford, C., Jones, C.D., Lowe, J.A., Meinshausen, M., Meinshausen, N., 2009. Warming caused by cumulative carbon emissions towards the trillionth tonne. *Nature* 458 (7242), 1163–1166. <https://doi.org/10.1038/nature08019>.
- Climate System Analysis Group. (n.d.). Big Six Monitor - Current and Projected State of the Western Cape dams. Retrieved April 2, 2019, from <http://cip.csag.uct.ac.za/monitoring/bigsix.html>.
- DEWA. (2018). DEWA sustainability report 2018. Dubai Electricity & Water Authority. Cape Town Department of Water & Sanitation, 2018. *Water Outlook 2018 Report*. City of Cape Town.
- Ding, K., Gilligan, J.M., Hornberger, G.M., 2019. Avoiding “Day-Zero”: a testbed for evaluating integrated food–energy–water management in Cape Town, South Africa. In: *Proceedings of the Winter Simulation Conference 2019*. IEEE.
- Ding, K., Gunda, T., Hornberger, G.M., 2019. Prominent influence of socioeconomic and governance factors on the food–energy–water nexus in Sub-Saharan Africa. *Earth's Future*.
- Elsawah, S., Filatova, T., Jakeman, A.J., Kettner, A.J., Zellner, M.L., Athanasiadis, I.N., et al., 2020. Eight grand challenges in socio-environmental systems modeling. In: *Socio-Environ. Syst. Model.*, 2, p. 16226. <https://doi.org/10.18174/semo.2020a16226>.
- Goodwin, P., Williams, R.G., Ridgwell, A., 2015. Sensitivity of climate to cumulative carbon emissions due to compensation of ocean heat and carbon uptake. *Nat. Geosci.* 8 (1), 29–34. <https://doi.org/10.1038/geo2304>.
- Hausfather, Z., Peters, G.P., 2020. Emissions – the ‘business as usual’ story is misleading. *Nature* 577 (7792), 618–620. <https://doi.org/10.1038/d41586-020-00177-3>.
- Heard, B.R., Miller, S.A., Liang, S., Xu, M., 2017. Emerging challenges and opportunities for the food–energy–water nexus in urban systems. *Current Opin. Chem. Eng.* 17, 48–53. <https://doi.org/10.1016/j.coche.2017.06.006>.
- Hyun, J.-Y., Huang, S.-Y., Yang, Y.C.E., Tidwell, V., Macknick, J., 2019. Develop a coupled agent-based modeling approach for uncertain water management decisions. *Hydrol. Earth Syst. Sci. Discuss.* 24 (2), 1–51. <https://doi.org/10.5194/hess-2018-555>.
- Kanta, L., Zechman, E., 2014. Complex adaptive systems framework to assess supply-side and demand-side management for urban water resources. *J. Water Resour. Plan. Manag.* 140 (1), 75–85. [https://doi.org/10.1061/\(ASCE\)WR.1943-5452.0000301](https://doi.org/10.1061/(ASCE)WR.1943-5452.0000301).
- Kretzmann, 2019. Retrieved May 25, 2020, from <https://www.groundup.org.za/article/cape-towns-groundwater-polluted/>.
- Lant, C., Baggio, J., Konar, M., Mejia, A., Ruddell, B., Rushforth, R., et al., 2019. The U.S. food–energy–water system: A blueprint to fill the mesoscale gap for science and decision-making. *Ambio* 48 (3), 251–263. <https://doi.org/10.1007/s13280-018-1077-0>.
- Naik, M., Abiodun, B.J., 2019. Projected changes in drought characteristics over the Western Cape, South Africa. *Meteorol. Appl.* (November 2018), 1–14. <https://doi.org/10.1002/met.1802>.
- Ozturk, I., 2017. The dynamic relationship between agricultural sustainability and food–energy–water poverty in a panel of selected Sub-Saharan African Countries. *Energy Policy* 107 (February), 289–299. <https://doi.org/10.1016/j.enpol.2017.04.048>.
- PUB, 2020. Desalinated Water. Singapore Ministry of Sustainability and the Environment. Retrieved June 1, 2020, from: <https://www.pub.gov.sg/watersupply/fournationaltaps/desalinatedwater>.
- Ritchie, J., Dowlatabadi, H., 2017. The 1000 GtC coal question: are cases of vastly expanded future coal combustion still plausible? *Energy Econ.* 65, 16–31. <https://doi.org/10.1016/j.eneco.2017.04.015>.
- Shumilova, O., Tockner, K., Thieme, M., Koska, A., Zarfl, C., 2018. Global water transfer megaprojects: a potential solution for the water-food-energy nexus? *Front. Environ. Sci.* 6 (DEC), 150. <https://doi.org/10.3389/fenvs.2018.00150>.
- Sieff, K., 2018. Cape Town’s water crisis is revealing South Africa’s inequality - The Washington Post. The Washington Post. Retrieved from. https://www.washingtonpost.com/news/world/wp/2018/02/23/feature/as-cape-towns-water-runs-out-there-rich-drill-wells-the-poor-worry-about-eating/?noredirect=on&utm_term=.7c37d8ae4d88.
- Sušnik, J., 2018. Data-driven quantification of the global water-energy-food system. *Resour. Conserv. Recycl.* 133 (November 2017), 179–190. <https://doi.org/10.1016/j.resconrec.2018.02.023>.
- Tafirenyika, M., 2018. Cape Town water taps running dry. Retrieved from. <https://www.un.org/africarenewal/magazine/april-2018-july-2018/cape-town-water-taps-running-dry>.
- United Nations, 2018. 68% of the World Population Projected to Live in Urban Areas by 2050, Says UN | UN DESA | United Nations Department of Economic and Social Affairs. Retrieved June 1, 2020, from. <https://www.un.org/development/desa/en/news/population/2018-revision-of-world-urbanization-prospects.html>.
- Villarroel Walker, R., Beck, M.B., Hall, J.W., Dawson, R.J., Heidrich, O., 2014. The energy–water–food nexus: Strategic analysis of technologies for transforming the urban metabolism. *J. Environ. Manag.* 141, 104–115. <https://doi.org/10.1016/j.jenvman.2014.01.054>.
- Visser, W.P., 2018. A perfect storm: the ramifications of Cape Town’s drought crisis. *J. Transdiscipl. Res. Southern Afr.* 14 (1), 1–10. <https://doi.org/10.4102/tdr.v14i1.567>.
- Walters, 2019. Retrieved May 26, 2020, from <https://calmatters.org/environment/2019/05/future-of-california-water-supply/>.
- Wang, Y., Zhou, Y., Franz, K., Zhang, X., Jack, K., Jia, G., 2021. Resources, conservation & recycling an agent-based framework for high-resolution modeling of domestic water use. *Resour. Conserv. Recycl.* 169 (November 2020), 105520. <https://doi.org/10.1016/j.resconrec.2021.105520>.
- Yang, J., Yang, Y.C.E., Khan, H.F., Xie, H., Ringler, C., Ogilvie, A., et al., 2018. Quantifying the sustainability of water availability for the water–food–energy–ecosystem nexus in the Niger River Basin. *Earth's Fut.* 6 (9), 1292–1310. <https://doi.org/10.1029/2018EF000923>.
- Zaman, K., Shamsuddin, S., Ahmad, M., 2017. Energy–water–food nexus under financial constraint environment: good, the bad, and the ugly sustainability reforms in sub-Saharan African countries. *Environ. Sci. Pollut. Res.* 24 (15), 13358–13372. <https://doi.org/10.1007/s11356-017-8961-1>.
- Zhang, P., Zhang, L., Chang, Y., Xu, M., Hao, Y., Liang, S., et al., 2019. Food–energy–water (FEW) nexus for urban sustainability: a comprehensive review. *Resour. Conserv. Recycl.* 142 (July 2018), 215–224. <https://doi.org/10.1016/j.resconrec.2018.11.018>.